Enhancement of Acylcarnitine Levels in Small Intestine of Abdominal Irradiation Rats Might Relate to Fatty Acid β-Oxidation Pathway Disequilibration

Hai-Xiang Liu[1], **Xue Lu**[1], **Hua Zhao**[1] , **Shuang Li**[1], **Ling Gao**[1] , **Mei Tian**[1] and **Qing-Jie Liu**[1]

Abstract

Objective: This study aims to analyze the alteration of carnitine profile in the small intestine of abdominal irradiation-induced intestinal injury rats and explore the possible reason for the altered carnitine profile.

Methods: The abdomens of 15 male Sprague Dawley (SD) rats were irradiated with 0, 10, and 15 Gy of ^{60}Co gamma rays. The carnitine profile in the small intestine and plasma samples of SD rats at 72 h after abdominal irradiated with 0 Gy or 10 Gy of ^{60}Co gamma rays were measured by targeted metabolomics. The changes of fatty acid β-oxidation (FAO), including the expression of carnitine palmitoyltransferase 1 (CPT1) and acyl-CoA dehydrogenases, were analyzed in the small intestine samples of SD rats after exposed to 0, 10, and 15 Gy groups.

Results: There were eleven acylcarnitines in the small intestine and fourteen acylcarnitines in the plasma of the rat model significantly enhanced, respectively (P < .05). The expression level and activity of CPT1 in the small intestine were remarkably increased (P < .05), and the activity of acyl-CoA dehydrogenase in the small intestine was noticeably reduced (P < .01) after abdominal irradiation.

Conclusion: The enhanced acylcarnitine levels in the small intestine of abdominal irradiation rats might relate to the FAO pathway disequilibration.

Introduction

As a potential approach of radiation biodosimetry, radiation metabolomics was initiated to measure the biological responses to radiation dose in the past few years.[1,2] These studies have found a large number of new promising candidate indicators of radiation exposure.[3] Among these indicators, the free L-carnitine and acylcarnitines were found altered in the serum, plasma, or urine of rodents,[2,4,5] non-human primates,[6,7] and humans[8,9] after radiation exposure. Due to the different analyzed instruments, samples, timing, and detection methods in these studies, the significantly differentiated carnitines were not same. However, most of the carnitine and acylcarnitines were elevated after irradiation. The reason for carnitine profile alteration after radiation exposure is urgent to be systematically explored.

[1]China CDC Key Laboratory of Radiological Protection and Nuclear Emergency, National Institute for Radiological Protection, Chinese Center for Disease Control and Prevention, Beijing, China

Corresponding Author:
Qing-Jie Liu, China CDC, National Institute for Radiological Protection, 2 Xinkang Street, Deshengmenwai, Beijing 100088, China.
Email: liuqingjie@nirp.chinacdc.cn

It was known that except for a few odd-chain acylcarnitines were derived from intermediates of amino acid catabolism, most of even-chain acylcarnitines were derived from fatty acid β-oxidation (FAO) pathway.[10] The altered acylcarnitines in the serum, plasma, or urine of animals and humans may be related to the changes of the FAO pathway after irradiation.[2,11]

In previous studies, the changed carnitine and acylcarnitines were identified mostly in blood or urine based on whole-body irradiation animal models. Knowledge of carnitine and acylcarnitines alteration in different organs or tissues based on whole-body irradiation models is inadequate. There is no study on intestinal carnitine alteration based on partial body irradiation models up till now. Only one study displayed that the long-chain acylcarnitines in multiple tissue types of non-human primates, including heart, lung, jejunum, spleen, liver, and kidney, were obviously increased after total body irradiation.[12] The carnitine profile may depend on the type of radiation and the sensitivity of different tissues and organs. Therefore, it is necessary to analyze the changes of carnitine profile in specific tissues or organs, which may be very helpful to elucidate the mechanism of radiation-induced sensitive tissue injury in the future.

The small intestine is much sensitive to radiation, due to its high proliferation rate.[13] Ionizing irradiation-induced toxic effect in the intestine is largely defined as intestinal stem cell death and apoptosis, insufficient replacement of villus epithelium, mucosal barrier breakdown, systemic infection, and in extreme cases, septic shock and death.[14,15] The toxic side effects of ionizing irradiation on cancer patients, including anorexia, vomiting, diarrhea, and dehydration, make the small intestine a dose-limiting organ both in total body and abdominopelvic radiation therapy procedures.[16,17] Radiation therapy (RT) plays an important role in the treatment of a wide variety of cancer, and in some cases, it has been proven the single best therapeutic approach.[18] Partial body irradiation is more widely applied in RT for cancer patients than total body irradiation. It is estimated that more than 200000 patients in the USA accept abdominopelvic RT each year, and the number of cancer survivors with post-radiation intestinal dysfunction is estimated to be $1.5-2$ million.[19] With increasing survival rates of cancer patients who have received abdominopelvic RT, more patients might be suffered from radiation-induced intestinal injury.[20,21] It is essential to understand the cell biology and molecular physiological status in radiation-induced intestinal injury from a new perspective, in order to provide new possible clues for the prevention of radiation-induced intestinal injury in near future.

In present study, an abdominal irradiation-induced intestinal injury model of rat was constructed. Then the alteration of carnitine profile in the small intestine and plasma in rat model at 72 h after 10 Gy of ^{60}Co gamma rays exposure was analyzed. Finally, the expression level or activity changes of components of FAO pathway, including the carnitine palmitoyltransferase 1 (CPT1), medium-chain acyl-CoA dehydrogenase (ACADM), and very-long-chain acyl-CoA dehydrogenase (ACADVL), were analyzed in the small intestine samples of the model.

Materials and Methods

Animals

Fifteen male Sprague Dawley (SD) rats ($180-220$ g) were used in this study. The use of animals and the study protocols were approved by the Experimental Animal Welfare Committee of National Institute for Radiological Protection (NIRP, act no. 2021-001), Chinese Center for Disease Control and Prevention. Fifteen rats were randomized into 3 groups and housed at a specific pathogen-free barrier area at the Department of Laboratory Animal Science, National Institute for Occupational Health and Poison Control (Beijing, China) under a relative humidity of $40-60\%$, the temperature at $20-24°C$, and with a 12 h/12 h light–dark cycle. The rats were fed with food and water *ad libitum*.

Abdominal Irradiation

Prior to irradiation, the rat was anesthetized with intraperitoneal injection sodium pentobarbital at 50 mg/kg body weight. The rat was irradiated with 0 Gy, 10 Gy, and 15 Gy of ^{60}Co gamma rays by a vertical radiation source (NIRP, Beijing, China). The irradiation was localized to a circle-shaped field of 3 cm × 3 cm encompassing the central abdominal region by using a 3-cm-thick lead shield to protect the rest of the body. The source–sample distance was 20 cm and the dose rate was .66 Gy/min. After irradiation, rats were returned to their cages with food and water *ad libitum*.

Hematoxylin and Eosin Staining of Rat Small Intestine

The rats from each group were sacrificed at 72 h after abdominal irradiation. The ileum samples were collected, fixed in 4% paraformaldehyde, and embedded in paraffin. Next, the samples were cut into 5 μm sections. After deparaffinized, the sections were stained with hematoxylin–eosin (H–E) and analyzed under a microscope. The histopathological alterations of mounted slides were assessed in a blinded manner by a histologist according to the method described in reference 22.

Measurement of Villous Length and Crypts to Villus Ratio

The villous length and crypts to villus ratio in rats were measured in a blinded manner from H–E-stained slides using SlideViewer software. The villous length in μm was determined from the base of each villus to the tip. The H–E-stained slides were further analyzed for crypts to villus ratio. Ten villi were respectively analyzed for villous length and crypts to villus ratio of each rat.

Targeted Metabolomics Analysis

The whole blood samples were collected from the heart of each SD rat after abdominal irradiation with 0 Gy or 10 Gy of ^{60}Co gamma rays. Then they were centrifuged at 3000× g for 10 min

to obtain plasma samples. The concentrations of carnitines in plasma and small intestine samples of SD rats were analyzed with the ultra-performance liquid chromatography-tandem mass spectrometry (UPLC-MS/MS) in positive electrosprays ionizing (ESI+) mode based on targeted metabolomics. The carnitines were quantified relative to deuterium-labeled carnitine and acylcarnitines (Cambridge Isotope Laboratories, USA) employing multiple reaction monitoring (MRM) transitions. The chromatographic separation was carried out on the UPLC I-Class system (Waters, USA) equipped with the ACQUITY UPLC high strength silica (HSS) T3 column (Waters, USA). The mobile phase consisted of solvent A (.1% formic, water) and solvent B (acetonitrile) with gradient elution. The flow rate of the mobile phase was .3 mL/min. The column temperature was maintained at 50°C. The injection volume was 5 μL. MRM analyses were performed using a TQ-XS triple quadrupole tandem mass spectrometer (Waters, USA). The ESI+ source temperature was 150°C, the capillary voltage was 2.5 kV, and the cone voltage was 20 V. The LC-MS system was controlled by Masslynx software, and data were collected and processed with the same software.

Quantitative Real-Time Polymerase Chain Reaction (qRT-PCR)

Total RNA of the small intestine samples of SD rats were homogenized and isolated with TRIzol reagent (Ambion, USA) and then reverse transcribed into cDNA using the Primescript RT reagent kit (Takara, Japan). The quantitative real-time polymerase chain reaction (qRT-PCR) was conducted with SYBR® green supermix kit (Bio-Rad Laboratories, USA) and ABI 7500 Real-Time PCR System (Applied Biosystems, USA). The β-actin was used as an endogenous control. The relative expression levels of the target genes were calculated by the $2^{-\Delta\Delta Ct}$ method. The gene-specific forward and reverse primers were as follows:

For CPT1A, Forward: 5′-CCTACCACGGCTGGATGTTT-3′, Reverse: 5′-TACAACATGGGCTTCCGACC-3′; For CPT1B, Forward: 5′-ACAGGCATAAGGGGTGGCAT-3′, Reverse: 5′-CACTCCAATCCCACCTCGACC-3′; For ACADM, Forward: 5′-GTCCTTGGCCCCGAATTGT-3′, Reverse: 5′-AGTTCTTTCGTGACAGGCTACC-3′; For ACADVL, Forward: 5′-CCCTAGCAGGCACCATGAAA-3′, Reverse: 5′-GCTTTTCCTGGATCACCCCA-3′.

Western Blot Analysis

The small intestine samples of SD rats were collected at 72 h after abdominal irradiation with 0 Gy, 10 Gy, and 15 Gy of ^{60}Co gamma rays and homogenized in ice-cold radioimmunoprecipitation assay (RIPA) buffer (Beyotime, China). The homogenate tube was placed into an ice bath and an ultrasonic cell dismembrator was used to interrupt the ultrasound for 5 s 5–6 times, and then the homogenate

was centrifuged with 140 00× g for 10 min at 4°C. The supernatant was collected and the concentrations of proteins were measured by a bicinchoninic acid protein assay (BCA) kit (Thermo Fisher, USA). 100 μg of protein was loaded into each lane, separated on SDS-PAGE, and transferred to polyvinylidene difluoride (PVFD) membrane and then immunoblotted with antibodies following the manufacturer's instruction. Immunoreactive bands were visualized using the ChemiDoc XRS system with Image Lab software (Bio-Rad, USA). Antibodies against CPT1A and β-actin were purchased from Proteintech (USA), antibody against CPT1B was purchased from Novus (USA), and anti-normal rabbit IgG and anti-normal mouse IgG were purchased from ZSGB (China).

Carnitine Palmitoyltransferase 1 Activity Assay in Rat Small Intestine Samples

The CPT1 enzymatic activities of the small intestine samples of SD rats, which were collected at 72 h after abdominal irradiation with 0 Gy, 10 Gy, and 15 Gy of ^{60}Co gamma rays, were measured following the instruction of the CPT1 activity kit (QIYI, China). In brief, the activity was analyzed by detecting the release levels of thiol coenzyme A (CoA-SH) from palmitoyl-CoA. After the released CoA-SH reacted with general thiol reagent 5, 5'-dithiobis-2-nitrobenzoic acid, yellow 2-nitro-5-thiobenzoic acid was produced. The change of absorption peak value at 412 nm in samples was used to quantitatively measure the activity of CPT1.

Fatty Acid Oxidation Rate Assay in Rat Small Intestine Samples

A total of 100 mg small intestine samples of SD rats, which were collected at 72 h after abdominal irradiation with 0 Gy, 10 Gy, and 15 Gy of ^{60}Co gamma rays, were homogenized. Mitochondria were isolated with the mitochondrial extraction kit (Solarbio, China). The concentrations of the mitochondrial proteins were detected by the BCA kit. The FAO rate of the sample was detected with the FAO kit (Genmed Scientifics, China).[23] The FAO rate was defined as micromoles ferricyanide reduction per min per milligram of protein, which represents total enzyme activity of acyl-CoA dehydrogenases, including the ACADM and ACADVL.

Statistical Analysis

Statistical differences among groups were analyzed by one-way analysis of variance (ANOVA) followed with least significant difference (LSD) *t*-tests or two-tailed Student's *t*-test was used for comparison of 2 groups. Data were expressed as mean ± SEM. A value of $P < .05$ was considered as statistically significant.
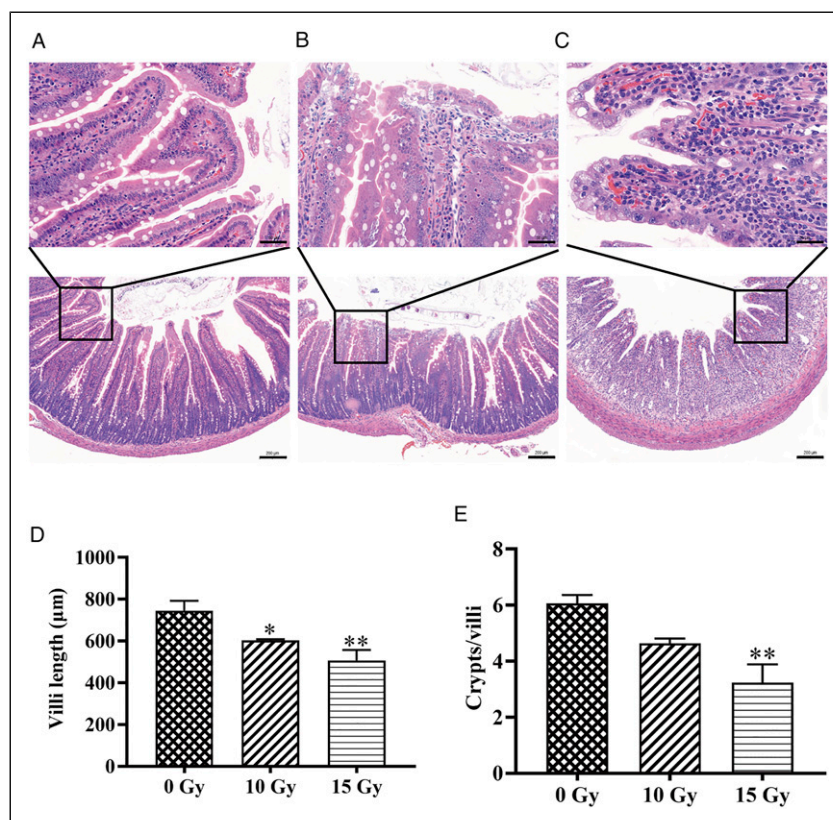
Figure 1. Establishment of an abdominal irradiation-induced intestinal injury model of Sprague Dawley (SD) rats (n = 3 rats per group). Representative hematoxylin and eosin (H–E) staining images of the small intestine of SD rats at 72 h after abdominal irradiated with 0 Gy (A), 10 Gy (B), or 15 Gy (C) of ^{60}Co gamma rays. Increased magnifications of square areas are shown. Scale bar = 200 μm (lower panel) and scale bar = 50 μm (upper panel). (D) Villous length of the small intestine from rats in panels A–C. (E) Crypts to villus ratio of the small intestine from rats in panels A–C. Ten villi were respectively analyzed for villous length and crypts to villus ratio of each rat. Data represent mean ± SEM (*P < .05, **P < .01, compared with the 0 Gy group, LSD *t*-test).

Results

Construction of SD Rat Model of Abdominal Irradiation-Induced Intestinal Injury

To investigate the effect of abdominal irradiation on the carnitine profile in the small intestine, male SD rats were locally abdominal exposed to 0 Gy, 10 Gy, and 15 Gy of ^{60}Co gamma rays. The small intestine tissues were collected at 72 h after abdominal irradiation, and the pathological changes of intestinal tissue were evaluated by H–E staining. The small intestine from the 0 Gy group exhibited a normal histological structure (Figure 1A). In the 10 Gy group, the villi and mucosa structure of the small intestine samples were damaged, there were edema, inflammatory cell infiltration, and capillary dilatation hyperemia in the epithelial submucosa; the epithelial surface shedding and micro-ulcers were observed (Figure 1B); the villous length in the 10 Gy group was significantly decreased compared with those in the 0 Gy group (P < .05, Figure 1D). The villus and mucosa structure of the small intestine samples in the 15 Gy group also showed similar morphologic changes; the changes of edema, inflammatory cell infiltration,

and capillary dilatation hyperemia were more obvious (Figure 1C); the villous length and as well as crypts to villus ratio in the 15 Gy group were significantly decreased compared with those in the 0 Gy group (P < .01, Figure 1D and E). These pathological changes in small intestine samples from 10 Gy and 15 Gy groups proved that the abdominal irradiation-induced intestinal injury rat model was successfully constructed.

Acylcarnitines Enhancement in the Small Intestine of Rats After Abdominal Irradiation Exposure

The variation of carnitine profile in the small intestine tissue of the rats at 72 h after abdominal irradiated with 0 Gy or 10 Gy of ^{60}Co gamma rays was measured with targeted metabolomics. A visible carnitine profile difference in the small intestine between 10 Gy and 0 Gy groups was observed in the heatmap (Figure 2A). Among thirty-seven kinds of measured carnitines in the small intestine tissue, eleven kinds of carnitines from the 10 Gy group were significantly enhanced compared with those from the 0 Gy group (P < .05, Figures 2B and C). Except for free L-carnitine (C0), the rest significantly
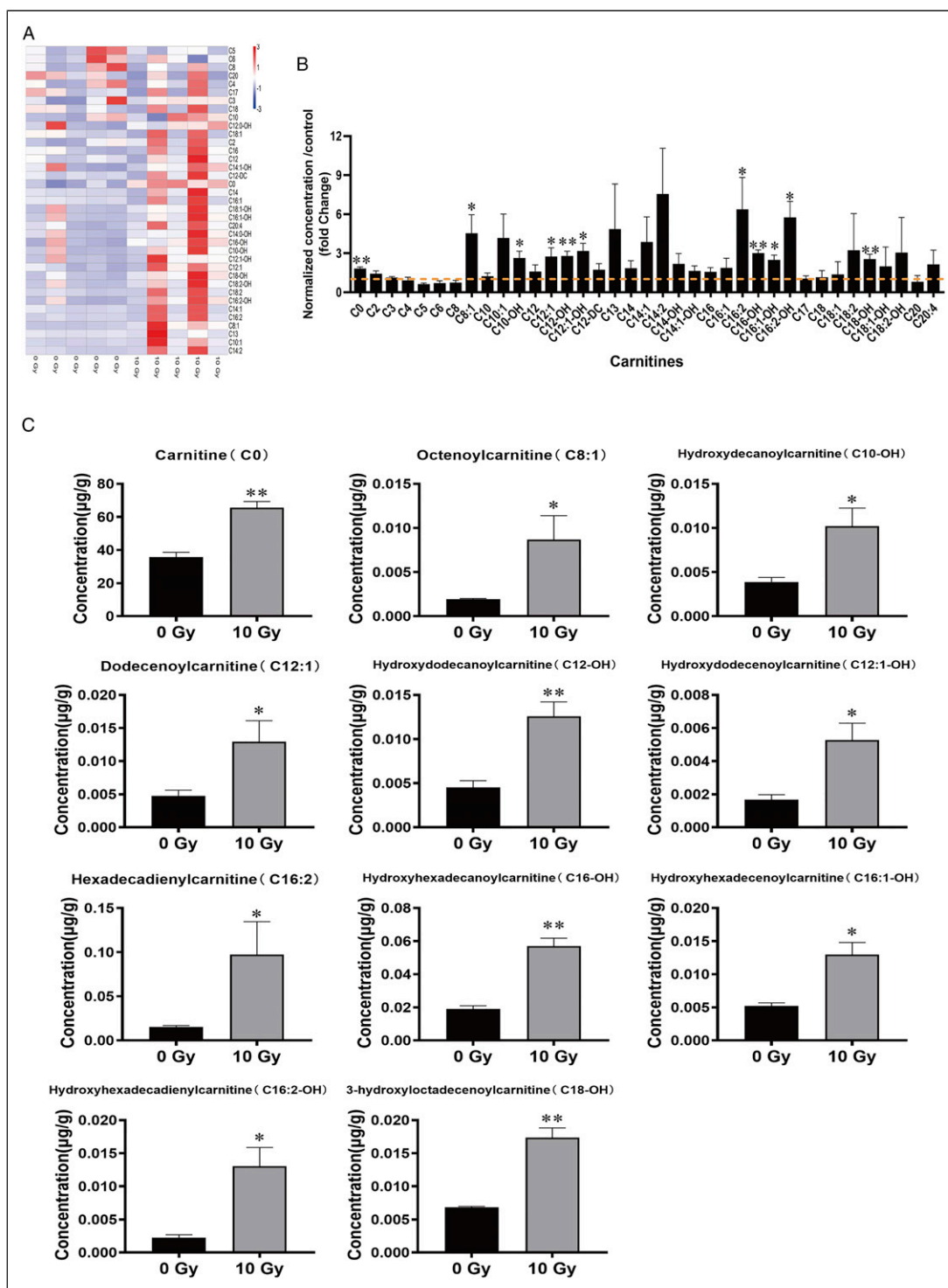
Figure 2. Changes of carnitine profile in the small intestine of SD rats abdominal irradiated with 10 Gy of ^{60}Co gamma rays (n = 5 rats per group). (A) Heatmap of carnitines in the plasma of SD rats at 72 h after abdominal irradiated with 0 Gy or 10 Gy of ^{60}Co gamma rays measured by targeted metabolomics. The heatmap showed the changes in the abundance of C0 to C20 carnitines after irradiation. Different colors represented the relative concentration (red and blue colors represented high and low concentration, respectively). (B) Fold changes of the multiple carnitines in the small intestine of rats in panel A. (C) The concentration of the carnitines in the small intestine of rats in panel A. Data represent mean ± SEM (*P < .05, **P < .01, compared with 0 Gy group, two-tailed Student's *t*-test).
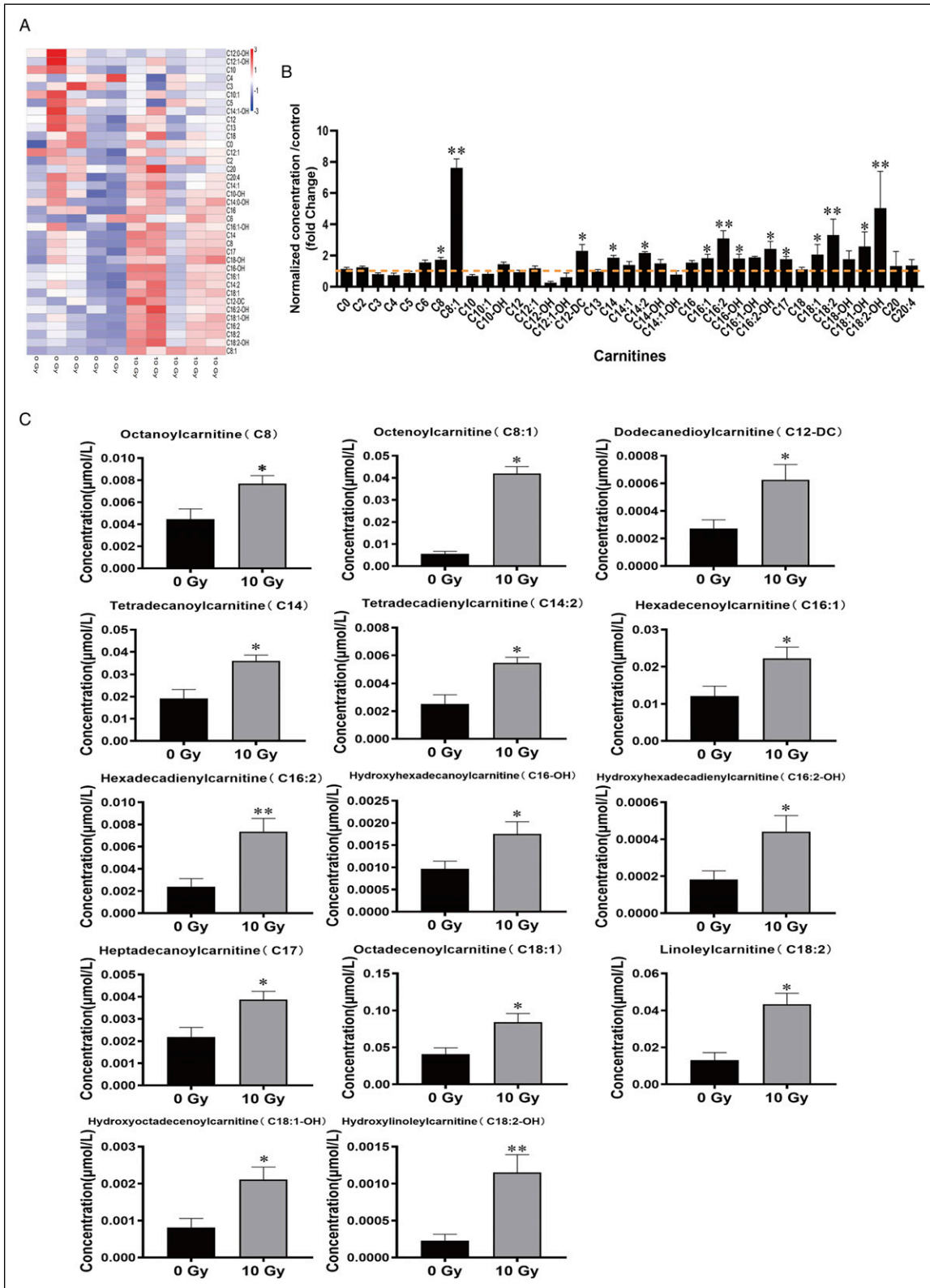
Figure 3. Changes of carnitine profile in the plasma of SD rats abdominal irradiated with 10 Gy of ^{60}Co gamma rays (n = 5 rats per group). (A) Heatmap of carnitines in the plasma of SD rats at 72 h after abdominal irradiated with 0 Gy or 10 Gy of ^{60}Co gamma rays measured by targeted metabolomics. (B) Fold changes of the multiple carnitines in the plasma of rats in panel A were calculated by dividing the concentrations of the carnitines in the 10 Gy group by those in the 0 Gy group. (C) The concentration of the carnitines in the plasma of rats in panel A. Data represent mean ± SEM (*P < .05, **P < .01, compared with the 0 Gy group, two-tailed Student's *t*-test).

enhanced acylcarnitines were all medium- or long-chain acylcarnitine (C8–C18).

Acylcarnitines Enhancement in the Plasma of Rat After Abdominal Irradiation Exposure

To explore whether the enhanced acylcarnitines in rat small intestine could be reflected in the plasma, the variation of carnitine profile in rat plasma at 72 h after abdominal irradiated with 0 Gy or 10 Gy of ^{60}Co gamma rays were also measured with targeted metabolomics. A visible carnitine profile change in rat plasma between 10 Gy and 0 Gy groups was also observed in the heatmap, which was similar to that in the small intestine (Figure 3A). Fourteen kinds of carnitines from the 10 Gy group were significantly enhanced compared with those from the 0 Gy group (P < .05, Figures 3B and C). All of the significantly enhanced acylcarnitines were medium- or long-chain acylcarnitine (C8–C18). Notably, 3 kinds of long-chain acylcarnitines, hexadecadienylcarnitine (C16:2), hydroxyhexadecanoylcarnitine (C16-OH), and hydroxyhexadecadienylcarnitine (C16:2-OH) were simultaneously elevated in the small intestine and the plasma samples. Further analysis displayed that the fold changes of those 3 kinds of acylcarnitines in the small intestine samples were about twice of those in the plasma. The variation of the carnitine profile provided a metabolic signature that the FAO pathway may be changed in response to abdominal irradiation-induced intestinal injury.

Elevated CPT1 Gene Expression Level and Enzyme Activity in the Small Intestine Samples of SD Rats After Abdominal Irradiation Exposure

To explore the possible reason for ^{60}Co gamma rays induced the acylcarnitines enhancement, the gene expression levels and enzyme activities of CPT1A and CPT1B (the known rate-limiting enzyme of FAO pathway) in the small intestine samples of the rats were analyzed at 72 h after abdominal irradiated with 0, 10, and 15 Gy of ^{60}Co gamma rays. Results showed that the mRNA levels of CPT1A and CPT1B from 10 Gy and/or 15 Gy groups were substantially higher than those of 0 Gy group (P < .01, Figure 4A). The protein levels of CPT1A and CPT1B from 10 Gy and 15 Gy groups were both significantly elevated compared with those of the 0 Gy group (P < .05, Figures 4B and C). The relative enzymatic activities of CPT1 were also significantly enhanced after abdominal irradiated with 10 Gy and 15 Gy of ^{60}Co gamma rays (P < .05, Figure 4D).

Decreased ACADM and ACADVL mRNA Levels and FAO Rate in the Small Intestine Samples of SD Rats After Abdominal Irradiation Exposure

As 2 enzymes in charge of catalyzing the first step of the fatty acids oxidation to produce electrons in the FAO pathway, the mRNA levels and enzyme activity of ACADM and ACADVL were also analyzed in this study. The mRNA levels of ACADM and ACADVL in the small intestine samples of the rats were detected at 72 h after local abdominal irradiated with 0, 10, and 15 Gy of ^{60}Co gamma rays. Compared to the 0 Gy group, the mRNA levels of ACADM and ACADVL were significantly reduced in 15 Gy groups (P < .05, Figure 5A). The enzymatic activity of the ACADM and ACADVL can be reflected with the rate of electron generation captured with ferricyanide in the FAO rate kit. The results showed that the FAO rate, representing total enzyme activity of acyl-CoA dehydrogenases, including the ACADM and ACADVL, was significantly decreased in the small intestine from 10 Gy and 15 Gy groups compared with those from the 0 Gy group (P < .01, Figure 5B).

Discussion

One review elaborated that even subtle alterations in metabolite products can be measured in biofluids, cells, and tissues that might discriminate physiological state changes before symptoms appear, due to the innate sensitivity of metabolomics.[24] They described that the combination of metabolomic, transcriptomic, and genomic analyses may allow ascertaining the mechanism underlying the phenotypic changes.[24] However, the present radiation metabolomics studies mainly focused on biomarker discovery; no study has explored the possible reason for the metabolic phenotype changes. Our study here correlates the carnitine profile with related pathway analysis to explore the possible reason for the altered carnitines in abdominal irradiation-induced intestinal injury.

In present study, an abdominal irradiation-induced intestinal injury model of rats was successfully constructed. The targeted metabolomics based on UPLC−MS/MS was conducted in the rat small intestine and plasma carnitine profile after exposure to 10 Gy of ^{60}Co gamma rays abdominal irradiation. Except for free L-carnitine and heptadecanoylcarnitine (C17), nearly all significantly enhanced acylcarnitines in the small intestine and plasma samples after abdominal irradiation were medium- and long even-chain acylcarnitines (C8–C18). Some previous studies also detected similar enhanced long-chain acylcarnitines, including palmitoylcarnitine (C16:0), sterearoylcarnitine (C18:0), octadecenoylcarnitine (C18:1), and linoleycarnitine (C18:2) in plasma or jejunum tissue after total body irradiation.[11,12,25] Perhaps due to different radiation types, animal models, or sampling times, and these studies were not limited to focus on the carnitine profile alteration, the discovered significant elevated long-chain acylcarnitines were not as numerous as those found in our study. Interestingly, 3 kinds of C16 species levels, including C16:2, C16-OH, and C16:2-OH, were simultaneously enhanced in the small intestine samples and the plasma. The fold changes of the 3 C16 species in the small intestine samples were more obvious than those in the plasma. These 3 kinds of C16 species might act as candidate markers
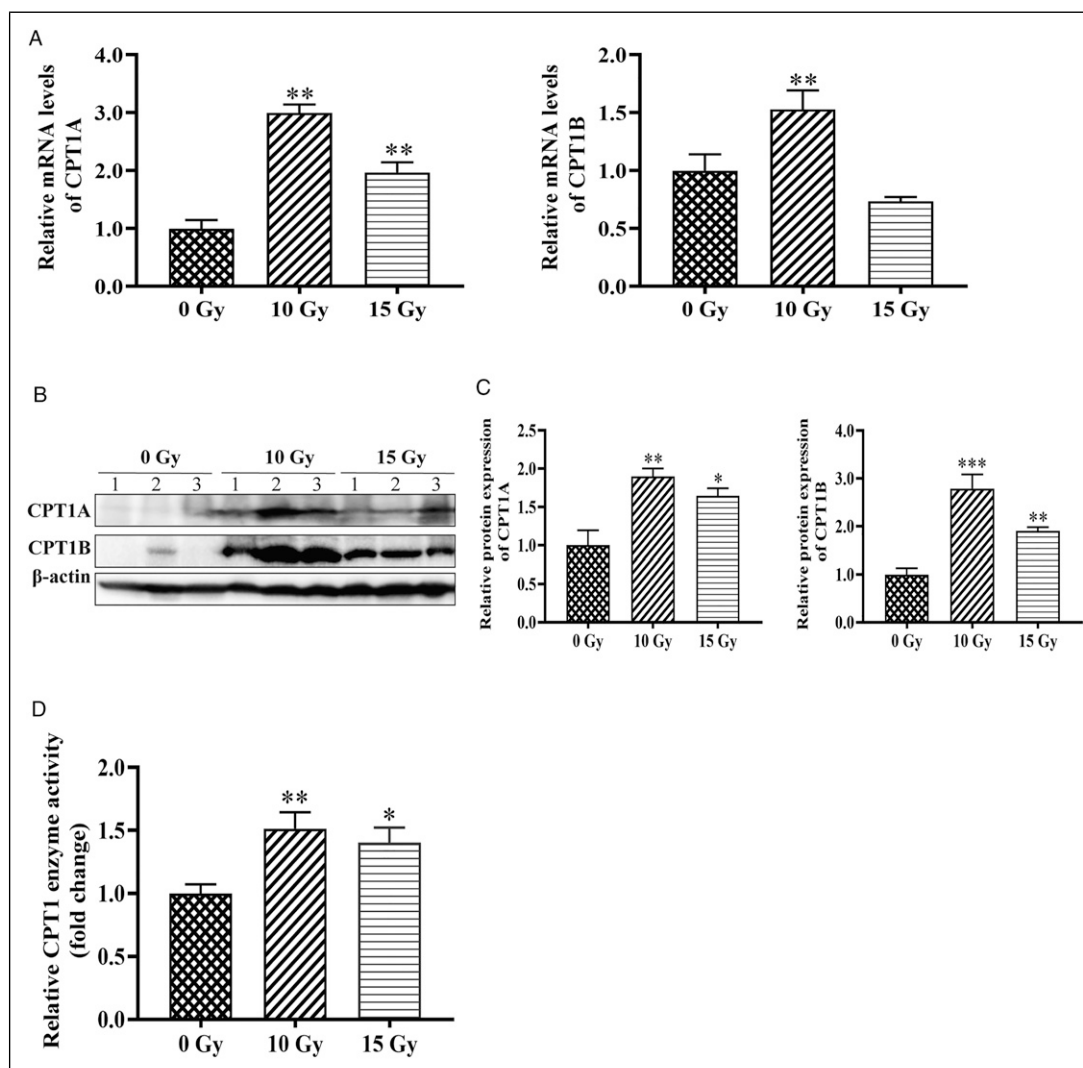
Figure 4. Changes of carnitine palmitoyltransferase 1 (CPT1) expression level and enzyme activity in the small intestine samples of SD rats after abdominal irradiated with 0 Gy, 10 Gy, or 15 Gy of ^{60}Co gamma rays (n = 3 rats per group). (A) The mRNA levels of CPT1 A and CPT1 B in the small intestine samples of SD rats were detected with real-time PCR at 72 h after abdominal irradiated with 0 Gy, 10 Gy, or 15 Gy of ^{60}Co gamma rays. (B, C) The protein levels of CPT1A and CPT1B in the small intestine samples of SD rats were detected with western blot and quantified by densitometry at 72 h after abdominal irradiated with 0 Gy, 10 Gy, or 15 Gy of ^{60}Co gamma rays. β-actin was used as a loading control. (D) The CPT1 enzymatic activities in the small intestinal homogenates of SD rats at 72 h after abdominal irradiated with 0 Gy, 10 Gy, or 15 Gy of ^{60}Co gamma rays. Results were presented as fold change in enzymatic activity in the 10 Gy or 15 Gy group relative to that in the 0 Gy group. Data represent mean ± SEM (*P < .05, **P < .01, ***P < .001, compared with 0 Gy group, LSD *t*-test).

for screening abdominal irradiation-induced intestinal injury from blood samples in the future.

The long-chain fatty acids in cytoplasm are transported into mitochondria exclusively as carnitine esters.[26] CPT1, the rate-limiting enzyme of FAO pathway, catalyzes the long-chain acyl-CoA and L-carnitine esterification reaction to form acylcarnitine. There are 3 subtypes of human CPT1, involving CPT1A, CPT1B, and CPT1C. Except for CPT1C, both CPT1A and CPT1B have acyltransferase activity.[27] The specific chain-length acyl-CoA in mitochondria is catalyzed dehydrogenation through acyl-CoA dehydrogenase of FAO pathway such as ACADVL and ACADM to finally produce an acyl-CoA with a specific two-carbon chain shortened. The changes of expression levels or activities of enzymes in FAO pathway may alter the carnitine profile.[28]

The plasma carnitine profile, which includes free carnitine and acylcarnitines, is frequently used for early detection of fatty acid oxidation disorders.[29] Recently, carnitine profile analysis has also been conducted to analyze disease processes induced by FAO pathway disequilibration, such as psoriasis[30] and maintenance hemodialysis patients.[31] CPT1 had been proved to play a crucial role in carnitine profile. The long-chain acylcarnitine levels were positively correlated with the activity of CPT1.[32,33] Knockdown CPT1A in cells could
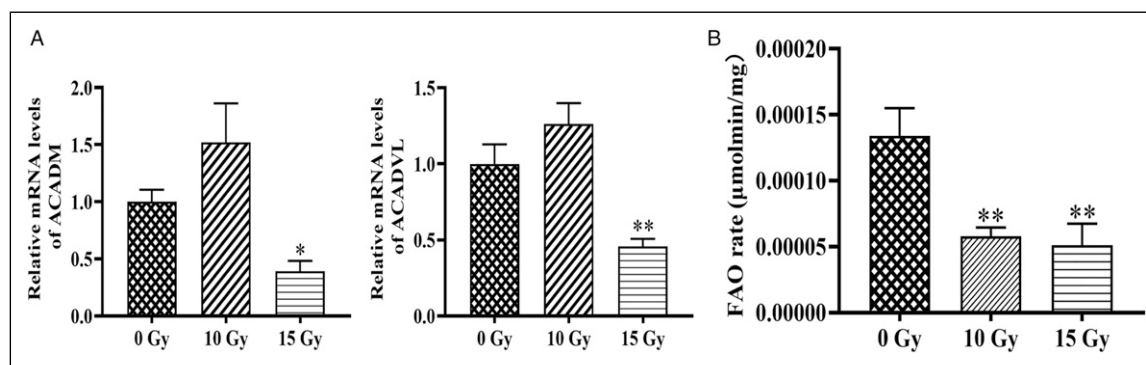
Figure 5. Changes of medium-chain acyl-CoA dehydrogenase (ACADM) and very-long-chain acyl-CoA dehydrogenase (ACADVL) mRNA levels and fatty acid β-oxidation (FAO) rate in the small intestine samples of SD rats abdominal irradiated with 0 Gy, 10 Gy, or 15 Gy of ^{60}Co gamma rays (n = 3 rats per group). (A) The mRNA levels of ACADM and ACADVL in the small intestine samples of SD rats were detected with real-time PCR at 72 h after abdominal irradiated with 0 Gy, 10 Gy, or 15 Gy of ^{60}Co gamma rays. (B) FAO rates in the small intestine samples of SD rats. This value represented the total enzyme activity of acyl-CoA dehydrogenases including ACADM and ACADVL. Data represent mean ± SEM (*P < .05, **P < .01, compared with the 0 Gy group, LSD *t*-test).

greatly downregulate the concentration of the medium- and long-chain acylcarnitine levels (C12, C14, and C16).[34] The C10- to C16-chain acylcarnitines were observed in cases of ACADVL deficiency.[35] The elevated C8-chain acylcarnitines were used to confirm ACADM deficiency.[36,37] The accumulation of the long-chain acylcarnitines in the small intestine and plasma samples of rats after abdominal irradiation may be caused by the alteration of gene expression levels or activities of enzymes in FAO pathway.

To our best knowledge, no study has shown direct evidence indicating that the FAO pathway was altered in normal tissues after total or partial body radiation exposure. There were only 2 studies verified that the CPT1A expression level was noticeably enhanced in the radio-resistance cells generated from parent cancer cells with continuous ionizing radiation.[34,38] In addition, some studies have discovered that radiation could robustly activate the adenosine monophosphate-activated kinase (AMPK), the upstream regulator of CPT1 enzyme activity, which indicated radiation may activate CPT1 by the pathway.[39,40] Our present study confirmed that the expression levels of CPT1A and CPT1B in the small intestine samples were obviously enhanced in the abdominal irradiation-induced intestinal injury rat model. Consistent with this, the activity of CPT1 enzyme was also dramatically improved in the 10 Gy and 15 Gy groups. These results indicated that abdominal irradiation indeed activated the CPT1 enzyme in FAO pathway.

Our study found that the mRNA levels of ACADM and ACADVL in the small intestine samples were remarkably reduced only in 15 Gy groups. The FAO rate, representing total enzyme activity of acyl-CoA dehydrogenases, including the ACADM and ACADVL, was dramatically dropped in both 10 Gy and 15 Gy groups. Compared with the mRNA levels of ACADM and ACADVL, the FAO rate in this study may be more sensitive to radiation exposure. This finding is consistent with some earlier studies of that ionizing radiation

could enhance the hyperacetylation levels of ACADVL and ACADM to reduce their activities in mice.[41,42]

These results indicated that the abdominal irradiation-induced increased medium- and long-chain acylcarnitines in the small intestine samples may be related to the FAO pathway disequilibration. The enhanced expression and activity of CPT1 in FAO pathway improved the levels of fatty acids transported into mitochondria,[33] and at the same time, the decreased activities of acyl-CoA dehydrogenases blocked the complete oxidation of the fatty acids in mitochondria, inducing accumulation of the medium- and long-chain acyl-carnitines in the small intestine samples, finally increasing the level of the metabolite in plasma. Notably, our study preliminarily indicated that the changes of carnitine profile in the small intestine of abdominal irradiation rats might relate to the FAO pathway disequilibration. However, there were more than ten kinds of enzyme involved in the FAO pathway, and the abnormities of other enzymes such as mitochondrial trifunctional protein can also result in the change of the carnitine profile. Our study only focused on the changes of several enzymes in the FAO pathway; systematic study would be conducted to elaborate the changes of other enzymes in the FAO pathway after irradiation in near future.

Conclusion

The targeted metabolomics based on UPLC−MS/MS platform was conducted to analyze the effect of abdominal irradiation on carnitine profile in the small intestine and plasma of rats 72 h after ^{60}Co gamma rays exposure. There were eleven acylcarnitines in the small intestine and fourteen acylcarnitines in the plasma of the abdominal irradiation-induced intestinal injury model significantly enhanced respectively. Most of the enhanced acylcarnitines were medium- or long-chain acylcarnitine (C8–C18). Importantly, this study indicated that the enhanced acylcarnitine levels in small

intestine of abdominal irradiation rats might relate to the FAO pathway disequilibration. Although the effect of the FAO pathway disequilibration on radiation damage needs further investigation, this study provides a new thought for exploring the reason for radiation-induced subtle alterations in metabolites, thus providing a new potential target for exploring the mechanism of radiation-induced injury.

Author Contributions

Hai-Xiang Liu and Qing-Jie Liu designed the study, wrote the manuscript, and were involved in revising the manuscript. Hai-Xiang Liu performed experiments with the help of Xue Lu, Hua Zhao, Shuang Li, and Ling Gao, and Mei Tian helped to analyze the data and prepare and revise the manuscript. All authors have approved the final version.

Declaration of Conflicting Interests

The author(s) declared no potential conflicts of interest with respect to the research, authorship, and/or publication of this article.

Funding

ORCID iDs

Hua Zhao https://orcid.org/0000-0002-1039-9073
Ling Gao https://orcid.org/0000-0002-1846-7106
Mei Tian https://orcid.org/0000-0003-2004-4302
Qing-Jie Liu https://orcid.org/0000-0002-7406-7414

References

1. Coy SL, Cheema AK, Tyburski JB, Laiakis EC, Collins SP, Fornace AJ. Radiation metabolomics and its potential in biodosimetry. *Int J Radiat Biol*. 2011;87(8):802-823.

2. Golla S, Golla JP, Krausz KW, et al. Metabolomic analysis of mice exposed to gamma radiation reveals a systemic understanding of total-body exposure. *Radiat Res*. 2017;187(5): 612-629.

3. Zhao H, Xi C, Tian M, et al. Identification of potential radiation responsive metabolic biomarkers in plasma of rats exposed to different doses of cobalt-60 gamma rays. *Dose-Response*. 2020; 18(4): 1559325820979570.

4. Goudarzi M, Weber WM, Mak TD, et al. A comprehensive metabolomic investigation in urine of mice exposed to strontium-90. *Radiat Res*. 2015;183(6):665-674.

5. Goudarzi M, Weber W, Mak TD, et al. Development of urinary biomarkers for internal exposure by cesium-137 using a metabolomics approach in mice. *Radiat Res*. 2014;181(1):54-64.

6. Pannkuk EL, Laiakis EC, Gill K, et al. Liquid chromatography-mass spectrometry-based metabolomics of nonhuman primates after 4 Gy total body radiation exposure: Global effects and targeted panels. *J Proteome Res*. 2019;18(5):2260-2269.

7. Pannkuk EL, Laiakis EC, Garcia M, Fornace AJ, Singh VK. Nonhuman primates with acute radiation syndrome: results from a global serum metabolomics study after 7.2 Gy total-body irradiation. *Radiat Res*. 2018;190(6): 576-583.

8. Ozmen HK, Erdemci B, Askin S, Sezen O. Carnitine and adiponectin levels in breast cancer after radiotherapy. *Open Med*. 2017;12(1):189-194.

9. Laiakis EC, Mak TD, Anizan S, et al. Development of a metabolomic radiation signature in urine from patients undergoing total body irradiation. *Radiat Res*. 2014;181(4):350-361.

10. Rinaldo P, Cowan TM, Matern D. Acylcarnitine profile analysis. *Genet Med*. 2008;10(2):151-156.

11. Pannkuk EL, Laiakis EC, Authier S, Wong K, Fornace AJ. Targeted metabolomics of nonhuman primate serum after exposure to ionizing radiation: Potential tools for high-throughput biodosimetry. *RSC Adv*. 2016;6(56):51192-51202.

12. Cheema AK, Mehta KY, Rajagopal MU, Wise SY, Fatanmi OO, Singh VK. Metabolomic studies of tissue injury in nonhuman primates exposed to Gamma-radiation. *Int J Mol Sci*. 2019; 20(13):3360.

13. Li M, Du A, Xu J, et al. Neurogenic differentiation factor NeuroD confers protection against radiation-induced intestinal injury in mice. *Sci Rep*. 2016;6:30180.

14. Hirama T, Tanosaki S, Kandatsu S, et al. Initial medical management of patients severely irradiated in the Tokai-mura criticality accident. *Br J Radiol*. 2003;76(904):246-253.

15. Hauer-Jensen M, Wang J, Denham JW. Bowel injury: current and evolving management strategies. *Semin Radiat Oncol*. 2003;13(3):357-371.

16. Zhang H, Yan H, Zhou X, et al. The protective effects of Resveratrol against radiation-induced intestinal injury. *BMC Compl Altern Med*. 2017;17(1):410.

17. Bhanja P, Norris A, Gupta-Saraf P, Hoover A, Saha S. BCN057 induces intestinal stem cell repair and mitigates radiation-induced intestinal injury. *Stem Cell Res Ther*. 2018;9(1):26.

18. Shadad AK, Sullivan FJ, Martin JD, Egan LJ. Gastrointestinal radiation injury: symptoms, risk factors and mechanisms. *World J Gastroenterol*. 2013;19(2):185-198.

19. Hauer-Jensen M, Wang J, Boerma M, Fu Q, Denham JW. Radiation damage to the gastrointestinal tract: mechanisms, diagnosis, and management. *Curr Opin Support Palliat Care*. 2007;1(1):23-29.

20. Arnold M, Rutherford MJ, Bardot A, et al. Progress in cancer survival, mortality, and incidence in seven high-income countries 1995-2014 (ICBP SURVMARK-2): a population-based study. *Lancet Oncol*. 2019;20(11):1493-1505.

21. Baskar R, Lee KA, Yeo R, Yeoh K-W. Cancer and radiation therapy: current advances and future directions. *Int J Med Sci*. 2012;9(3):193-199.

22. Andújar I, Recio MC, Giner RM, et al. Inhibition of ulcerative colitis in mice after oral administration of a polyphenol-enriched cocoa extract is mediated by the inhibition of STAT1 and STAT3

phosphorylation in colon cells. *J Agric Food Chem*. 2011;59(12): 6474-6483.

23. Xu Y, Huang J, Xin W, et al. Lipid accumulation is ahead of epithelial-to-mesenchymal transition and therapeutic intervention by acetyl-CoA carboxylase 2 silence in diabetic nephropathy. *Metabolism*. 2014;63(5):716-726.

24. Johnson CH, Ivanisevic J, Siuzdak G. Metabolomics: beyond biomarkers and towards mechanisms. *Nat Rev Mol Cell Biol*. 2016;17(7):451-459.

25. Zhao L, He X, Shang Y, et al. Identification of potential radiation-responsive biomarkers based on human orthologous genes with possible roles in DNA repair pathways by comparison between Arabidopsis thaliana and homo sapiens. *Sci Total Environ*. 2020; 702:135076.

26. Houten SM, Violante S, Ventura FV, Wanders RJA. The biochemistry and physiology of mitochondrial fatty acid β-oxidation and its genetic disorders. *Annu Rev Physiol*. 2016;78:23-44.

27. Houten SM, Wanders RJA. A general introduction to the biochemistry of mitochondrial fatty acid β-oxidation. *J Inherit Metab Dis*. 2010;33(5):469-477.

28. Hagenbuchner J, Scholl-Buergi S, Karall D, Ausserlechner MJ. Very long-/and long chain-3-hydroxy acyl coA dehydrogenase deficiency correlates with deregulation of the mitochondrial fusion/fission machinery. *Sci Rep*. 2018;8(1):3254.

29. Elizondo G, Matern D, Vockley J, Harding CO, Gillingham MB. Effects of fasting, feeding and exercise on plasma acylcarnitines among subjects with CPT2D, VLCADD and LCHADD/TFPD. *Mol Genet Metabol*. 2020;131(1-2):90-97.

30. Chen C, Hou G, Zeng C, Ren Y, Chen X, Peng C. Metabolomic profiling reveals amino acid and carnitine alterations as metabolic signatures in psoriasis. *Theranostics*. 2021;11(2):754-767.

31. Kamei Y, Kamei D, Tsuchiya K, Mineshima M, Nitta K. Association between 4-year all-cause mortality and carnitine profile in maintenance hemodialysis patients. *PLoS One*. 2018; 13(8):e0201591.

32. Heiner-Fokkema MR, Vaz FM, Maatman R, Kluijtmans LA, van Spronsen FJ, Reijngoud DJ. Reliable diagnosis of carnitine palmitoyltransferase type IA deficiency by analysis of plasma acylcarnitine profiles. *JIMD rep*. 2017;32:33-39.

33. Giordano A, Calvani M, Petillo O, et al. TBid induces alterations of mitochondrial fatty acid oxidation flux by malonyl-CoA-independent inhibition of carnitine palmitoyltransferase-1. *Cell Death Differ*. 2005;12(6):603-613.

34. Tan Z, Xiao L, Tang M, et al. Targeting CPT1A-mediated fatty acid oxidation sensitizes nasopharyngeal carcinoma to radiation therapy. *Theranostics*. 2018;8(9):2329-2347.

35. Yamada K, Taketani T. Management and diagnosis of mitochondrial fatty acid oxidation disorders: focus on very-long-chain acyl-CoA dehydrogenase deficiency. *J Hum Genet*. 2019; 64(2):73-85.

36. Anderson DR, Viau K, Botto LD, Pasquali M, Longo N. Clinical and biochemical outcomes of patients with medium-chain acyl-CoA dehydrogenase deficiency. *Mol Genet Metab*. 2020;129(1): 13-19.

37. Ibrahim S, Temtem T. *Medium-Chain Acyl-COA Dehydrogenase Deficiency*. StatPearls Publishing; 2021.

38. Han S, Wei R, Zhang X, et al. CPT1A/2-mediated FAO enhancement-a metabolic target in radioresistant breast cancer. *Front Oncol*. 2019;9, 1201.

39. Zannella VE, Cojocari D, Hilgendorf S, et al. AMPK regulates metabolism and survival in response to ionizing radiation. *Radiother Oncol*. 2011;99(3):293-299.

40. Sanli T, Rashid A, Liu C, et al. Ionizing radiation activates AMP-activated kinase (AMPK): a target for radiosensitization of human cancer cells. *Int J Radiat Oncol Biol Phys*. 2010;78(1): 221-229.

41. Barjaktarovic Z, Merl-Pham J, Braga-Tanaka I, et al. Hyperacetylation of cardiac mitochondrial proteins is associated with metabolic impairment and sirtuin downregulation after chronic total body irradiation of ApoE -/- mice. *Int J Mol Sci*. 2019; 20(20):5239.

42. Hirschey MD, Shimazu T, Goetzman E, et al. SIRT3 regulates mitochondrial fatty-acid oxidation by reversible enzyme deacetylation. *Nature*. 2010;464(7285):121-125.